Interaction of Transmission Network and Load Phasor Dynamics in Electric Power Systems

Eric H. Allen and M. D. Ilić

***Abstract*—This paper is concerned with modeling and analysis of an interconnected electric power system for frequency ranges in which phasor dynamics of transmission lines and loads may be important to include. In most studies, only phasor dynamics of generators are taken into account. Dynamics of all other system components (transmission lines, loads, and generator stator windings) are assumed stable and instantaneous (static). While several papers have examined phasor dynamics of the transmission lines, particularly when these are equipped with FACTS devices, no systematic investigation has been carried out concerning validity of static load models in this case. It is shown in this paper that problems may arise in particular when a static constant power load model is used at the same time that phasor dynamics of transmission lines are included. Standard singular perturbation-based arguments for neglecting load dynamics are shown not to be applicable in this case. More generally, the paper raises a general concern about consistency of electric power system models in frequency ranges where phasor dynamics of the devices typically assumed to be static must be taken into consideration.**

***Index Terms*—Electric power systems, flexible AC transmission systems (FACTS) control, load modeling, modeling, phasor dynamics.**

I. Introduction

A POWER system may be described as a combination of elements—generators, loads, and transmission lines—all of which are dynamic in nature. The collective dynamics of these various elements may be written mathematically as a set of ordinary differential equations (ODE's). For most dynamic studies, the dynamics of the transmission lines and the loads are neglected and replaced by a set of algebraic constraints. This substitution replaces the ODE description of the system with one consisting of differential-algebraic equations (DAE's) [1]. Although the substitution reduces the order of the system, DAE descriptions are in general harder to study and simulate than ODE's, and system control design is also harder.

Recently, the phasor-based modeling of the dynamics of the network components has been applied to the analysis of power systems phenomena, such as subsynchronous resonance [2]–[5]. Additions to the transmission grid, including series capacitor compensation and recent technological advances such as Flexible AC Transmission System (FACTS) controls, change the nature of the dynamics of the transmission lines. Given these changes and the difficulty with the DAE description of the system, it is often convenient to include the transmission line dynamics for simulations[1]; however, it is then necessary to also include dynamics of the loads as well. The combination of static load models with line dynamics often leads to some erroneous conclusions; more complete models of the load which include dynamic properties are therefore needed. For example, a load which has a shunt capacitor for reactive power balance may have dynamics which behave much differently from a simple series resistance and inductance. Most conventional load models [9], such as the ZIP model [10], do not provide a detailed or accurate description of the phasor dynamics, and hence do not model these fast dynamics in the power system adequately. Some dynamic load models [11], [12] which are used to study other phenomena are also unsuitable for the analysis of phasor dynamics.

In this paper, we examine how these network dynamics interact with two load models which represent two of the three components of the ZIP model. The first model is to treat the load as a constant impedance. The second model represents the load as a device which draws constant real and reactive power. The inclusion of the phasor dynamics leads to some interesting results regarding the viability of the constant power (PQ) load model. The combination of a constant current load (the third component of the ZIP model) with a transmission line in which the current is a state variable is not a well-posed problem when using phasor dynamics. A third load model which includes dynamics is also examined in order to provide some insight into the observed stability results of the two static load models.

As is well known, the constituent voltage-current relations for the basic circuit elements (R, L, and C respectively) in the time domain are

$$v_R(t) = Ri_R(t) \tag{1}$$

$$v_L(t) = L\frac{di_L(t)}{dt} \tag{2}$$

$$i_C(t) = C\frac{dv_C(t)}{dt}. \tag{3}$$

A phasor is simply a complex number which represents a voltage or current as a sinusoid with a magnitude and phase. Mathematically, the phasor $\hat{V}$ is related to the time domain $v(t)$ by

$$v(t) = \Re(\hat{V}e^{j\omega t}). \tag{4}$$

Note that a phasor carries no frequency information.

Manuscript received June 7, 1996; revised August 19, 1997 and July 12, 1998. This paper was recommended by Associate Editor A. Ioinovici.

The authors are with the Massachusetts Institute of Technology, Cambridge, MA 02139 USA (e-mail: ilic@mit.edu).

Publisher Item Identifier S 1057-7122(00)09912-8.

[1]In this paper only the lumped parameter representation of electric power system components is assumed. Phenomena for which truly distributed parameter modeling is required are treated elsewhere [6]–[8]. The issue of conditions under which lumped parameter modeling is valid is not a subject of this paper.

If we convert the basic circuit element equations (1)–(3) into phasor form by applying (4), we have

$$\hat{V}_R = \hat{Z}_R \hat{I}_R \tag{5}$$

$$\hat{V}_L = L\frac{d\hat{I}_L}{dt} + \hat{Z}_L \hat{I}_L \tag{6}$$

$$\hat{I}_C = C\frac{d\hat{V}_C}{dt} + \hat{Y}_C \hat{V}_C \tag{7}$$

where $\hat{Z}_R = R$, $\hat{Z}_L = j\omega L$, and $\hat{Y}_C = j\omega C$. For most power systems analysis, such as load flow, the time derivatives in these equations are assumed to be negligible and are ignored. However, in certain cases, such as subsynchronous resonance [13]–[15], these time derivatives are significant. For example, a 60-Hz phasor representation of a subsynchronous current of 30 Hz will include a time-varying component

$$i(t) = 5\cos 60\pi t \leftrightarrow \hat{I} = 5e^{-j60\pi t}. \tag{8}$$

Therefore, in these situations, the time derivatives can not be neglected.

This paper is organized as follows: Section II illustrates the phasor dynamics for the simple case of a single slack bus connected to one load of constant impedance by one transmission line. It will be seen that for this case, the phasor dynamics are always stable. Section III examines the dynamics for the same system, except that the constant impedance load is replaced by a constant PQ load. In this case, the phasor dynamics are not always stable. Section IV examines the phasor dynamics if the load is represented by a simple dynamic model. Section V examines all three types of load models in a three bus system with one generator and one slack bus. Finally, conclusions are drawn in Section VI.

II. Constant Impedance Load Model

The first system we will examine is shown in Fig. 1. It simply consists of a constant voltage source (infinite bus) connected to a load by a single transmission line. Using (6), the phasor dynamics of this system are

$$\hat{V}_1 = \hat{V}_L + L\frac{d\hat{I}}{dt} + (R + jX)\hat{I}. \tag{9}$$

The phasors may be represented by their real (r) and imaginary (i) parts

$$L\dot{I}_r = V_{r1} - V_{rL} - RI_r + XI_i \tag{10}$$

$$L\dot{I}_i = V_{i1} - V_{iL} - RI_i - XI_r. \tag{11}$$

We now consider the case where the load is of constant impedance. For simplicity, we assume the load is totally resistive; in Fig. 1, any reactance in the load can be lumped into the transmission reactance, resulting in the same dynamics as the situation with a resistive load. Since $\hat{V}_L = R_L\hat{I}$, the phasor dynamics for the system are

$$L\dot{I}_r = V_{r1} - R_L I_r - RI_r + XI_i \tag{12}$$

$$L\dot{I}_i = V_{i1} - R_L I_i - RI_i - XI_r. \tag{13}$$

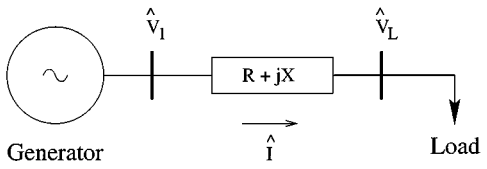

Fig. 1. System for analysis of phasor dynamics.

This is a linear system with system matrix

$$\mathbf{A} = \frac{1}{L}\begin{bmatrix} -(R_L + R) & X \\ -X & -(R_L + R) \end{bmatrix} \tag{14}$$

with eigenvalues

$$\lambda_{1,2} = -\frac{R_L + R}{L} \pm j\omega_0. \tag{15}$$

These roots always lie in the left half-plane (assuming $R > 0$, $X > 0$), and therefore we conclude that the phasor dynamics in connection with a constant impedance load are always stable.

III. Constant Power Load Model

We will now consider the phasor dynamics when the load is modeled as a constant PQ load. This model means that, for all time

$$\Re(\hat{V}_L\hat{I}^*) = V_{rL}I_r + V_{iL}I_i = P \tag{16}$$

$$\Im(\hat{V}_L\hat{I}^*) = V_{iL}I_r - V_{rL}I_i = Q. \tag{17}$$

Solving these two equations for V_{rL} and V_{iL} yields

$$V_{rL} = \frac{PI_r - QI_i}{I_r^2 + I_i^2} \tag{18}$$

$$V_{iL} = \frac{PI_i + QI_r}{I_r^2 + I_i^2}. \tag{19}$$

Therefore, with a constant power load, the phasor dynamics of (10) and (11) become

$$\dot{I}_r = \frac{1}{L}\left[V_{r1} - \frac{PI_r - QI_i}{I_r^2 + I_i^2} - RI_r + XI_i\right] \tag{20}$$

$$\dot{I}_i = \frac{1}{L}\left[V_{i1} - \frac{PI_i + QI_r}{I_r^2 + I_i^2} - RI_i - XI_r\right]. \tag{21}$$

This system is nonlinear. To determine stability around any equilibrium point, we find a small-signal linear model and evaluate the eigenvalues of the small-signal system. For the system of (20) and (21), the linearized small-signal model has a Jacobian of

$$\mathbf{A} = \begin{bmatrix} A_{11} & A_{12} \\ A_{21} & A_{22} \end{bmatrix} \tag{22}$$

$$A_{11} = \frac{\partial \dot{I}_r}{\partial I_r} = \frac{1}{L}\left[\frac{-P}{I_r^2 + I_i^2} + \frac{2I_r(PI_r - QI_i)}{(I_r^2 + I_i^2)^2} - R\right]$$

$$A_{12} = \frac{\partial \dot{I}_r}{\partial I_i} = \frac{1}{L}\left[\frac{Q}{I_r^2 + I_i^2} + \frac{2I_i(PI_r - QI_i)}{(I_r^2 + I_i^2)^2} + X\right]$$

$$A_{21} = \frac{\partial \dot{I}_i}{\partial I_r} = \frac{1}{L}\left[\frac{-Q}{I_r^2 + I_i^2} + \frac{2I_r(PI_i + QI_r)}{(I_r^2 + I_i^2)^2} - X\right]$$

$$A_{22} = \frac{\partial \dot{I}_i}{\partial I_i} = \frac{1}{L}\left[\frac{-P}{I_r^2 + I_i^2} + \frac{2I_i(PI_i + QI_r)}{(I_r^2 + I_i^2)^2} - R\right].$$

To complete the analysis, we note that the trace and determinant of $\mathbf{A}$ are

$$\mathrm{tr}(\mathbf{A}) = -\frac{2R}{L} \tag{23}$$

$$\det(\mathbf{A}) = \frac{1}{L^2}\left[R^2 + X^2 - \frac{P^2+Q^2}{(I_r^2+I_i^2)^2}\right]. \tag{24}$$

Since a 2×2 matrix has eigenvalues

$$\lambda_{1,2} = \frac{\mathrm{tr}(\mathbf{A}) \pm \sqrt{(\mathrm{tr}(\mathbf{A}))^2 - 4\det(\mathbf{A})}}{2} \tag{25}$$

the eigenvalues of $\mathbf{A}$ are then

$$\lambda_{1,2} = -\frac{R}{L} \pm \sqrt{\frac{P^2+Q^2}{L^2\left(I_r^2+I_i^2\right)^2} - \frac{X^2}{L^2}}. \tag{26}$$

Since $\mathrm{tr}(\mathbf{A}) < 0$, the system will be stable if $\det(\mathbf{A}) > 0$ at equilibrium, or equivalently

$$|\hat{V}_1 - \hat{V}_L| > |\hat{V}_L|. \tag{27}$$

To illustrate the preceding discussion, we will now present a numerical example and select typical values for the parameters. We choose $\hat{V}_1 = 1\angle 0°$, $R = 0.01, X = 0.1, P = 1$, and $Q = 0$. The two load flow solutions are the equilibria of the system; the first solution is $\hat{V}_L = 0.9847\angle -5.83°$, $\hat{I} = 1.016\angle -5.83°$ while solution #2 is $\hat{V}_L = 0.1021\angle -78.46°$, $\hat{I} = 9.798\angle -78.46°$. Note that solution 1 represents a desirable operating point (voltage magnitude near 1 p.u., small angle deviation) while the second solution is highly undesirable. Additionally, note that solution 1 corresponds to a constant impedance load with zero reactance and a resistance $R_L = 0.9696$.

Next, we evaluate the system matrix $\mathbf{A}$ for the small-signal model of (22) at each load flow solution point. At solution 1, we have

$$\mathbf{A} = \begin{bmatrix} 3542.1 & -361.6 \\ -1115.6 & -3617.5 \end{bmatrix}. \tag{28}$$

The eigenvalues of the matrix are

$$\lambda_1 = 3598.1 \quad \lambda_2 = -3673.4 \tag{29}$$

which clearly indicate that the system is unstable, even though the operating point is considered desirable. Note that $\hat{V}_1 - \hat{V}_L = 0.1021\angle 78.46°$; (27) indicates that solution 1 will be unstable.

At solution 2, the system matrix is

$$\mathbf{A} = \begin{bmatrix} -73.83 & 361.60 \\ -392.39 & -1.57 \end{bmatrix} \tag{30}$$

with eigenvalues

$$\lambda_1 = -37.70 + j374.94 \quad \lambda_2 = -37.70 - j374.94. \tag{31}$$

Although load flow solution 2 is clearly not a desired operating point for the system, the phasor dynamics around this point are in fact stable. Equation (27) is satisfied, as $\hat{V}_1 - \hat{V}_L = 0.9847\angle 5.83°$ at solution 2. Simulations of the system, as shown in Fig. 2, agree with the eigenvalue analysis. Starting at solution 1, the system states rapidly move away from the starting point and settle at solution 2.

IV. Dynamic Load Models

To illustrate the importance of the load dynamics, we will now consider a simple dynamic representation of the load as an admittance $G + jB$ where B is zero and G is a state variable with dynamics [16], [17]

$$\dot{G} = \frac{1}{\tau}\left[P - \frac{|\hat{I}|^2}{G}\right] \tag{32}$$

where τ is a fixed time constant. At equilibrium, the load consumes real power P; during transients, the conductance increases if the load uses less than P units of real power and vice versa.

The system dynamics of (10) and (11) now become

$$L\dot{I}_r = V_{r1} - \frac{I_r}{G} - RI_r + XI_i \tag{33}$$

$$L\dot{I}_i = V_{i1} - \frac{I_i}{G} - RI_i - XI_r \tag{34}$$

$$\dot{G} = \frac{1}{\tau}\left[P - \frac{I_r^2+I_i^2}{G}\right]. \tag{35}$$

The Jacobian of the system is

$$\mathbf{A} = \begin{bmatrix} -\dfrac{R+G^{-1}}{L} & \dfrac{X}{L} & \dfrac{I_r}{LG^2} \\ -\dfrac{X}{L} & \dfrac{R+G^{-1}}{L} & \dfrac{I_i}{LG^2} \\ -\dfrac{2I_r}{\tau G} & -\dfrac{2I_i}{\tau G} & \dfrac{I_r^2+I_i^2}{\tau G^2} \end{bmatrix}. \tag{36}$$

The stability of the system is very dependent on the time constant τ of the load. Note that the time constant of the phasor dynamics (denoted τ_{ph}) is

$$\tau_{ph} = \frac{L}{R+G^{-1}}. \tag{37}$$

Using the example parameters in the last section, τ_{ph} is on the order of 10^{-4} s. A much longer value for τ means that the phasor dynamics interact with a load that resembles a constant impedance. For example, if $\tau = 0.1$ s, the system eigenvalues at equilibrium are

$$\lambda_{1,2} = -3683.4 \pm j377.84 \quad \lambda_3 = -9.3471. \tag{38}$$

The first two eigenvalues correspond to the fast phasor dynamics; the third eigenvalue represents the much slower dynamics of the load conductance. If $\tau \gg \tau_{ph}$, the eigenvalues of (36) approach

$$\lambda_{1,2} = -\frac{R+G^{-1}}{L} \pm j\omega_0 \tag{39}$$

$$\lambda_3 = \frac{\left(I_r^2+I_i^2\right)\left[G((R+G^{-1})^2+X^2) - 2(R+G^{-1})\right]}{\tau G^3((R+G^{-1})^2+X^2)}. \tag{40}$$

If $G^{-2} > R^2 + X^2$, the load model will be stable for $\tau \gg \tau_{ph}$. Note that for a purely resistive load in Fig. 1, maximum real power transfer occurs when the load resistance equals $\sqrt{R^2+X^2}$. In most typical power systems, the load resistance is much larger than this value, and therefore the load model of (32) with a sufficiently large time constant τ is stable.

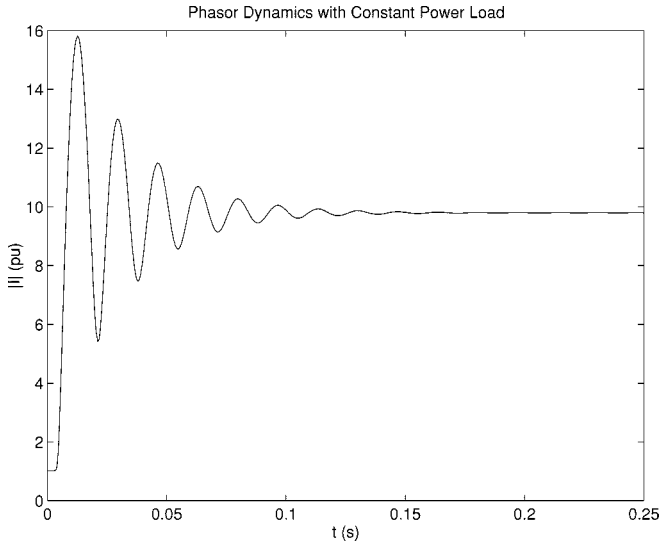

Fig. 2. Current magnitude with a constant power load.

On the other hand, if τ is much shorter than τ_{ph}, the load does not resemble a constant impedance, and the system becomes unstable. For $\tau = 10^{-7}$ s, the system eigenvalues are

$$\lambda_1 = 3600.8 \quad \lambda_2 = -3673.4 \quad \lambda_3 = 9.6885 \times 10^6. \tag{41}$$

For $0 < \tau \ll \tau_{ph}$, (36) has an eigenvalue of

$$\lambda_3 = \frac{|\hat{I}|^2}{\tau G^2} \tag{42}$$

which is always positive.

For completeness, we also consider a reversed version of the dynamic load, where

$$\dot{G} = \frac{1}{\tau}\left[\frac{|\hat{I}|^2}{G} - P\right]. \tag{43}$$

As with the preceding model, such a load may be implemented in principle by feedback control. The Jacobian of the system is now given by

$$\mathbf{A} = \begin{bmatrix} -\dfrac{R+G^{-1}}{L} & \dfrac{X}{L} & \dfrac{I_r}{LG^2} \\ -\dfrac{X}{L} & -\dfrac{R+G^{-1}}{L} & \dfrac{I_i}{LG^2} \\ \dfrac{2I_r}{\tau G} & \dfrac{2I_i}{\tau G} & -\dfrac{I_r^2+I_i^2}{\tau G^2} \end{bmatrix}. \tag{44}$$

For a fast time constant $(0 < \tau \ll \tau_{ph})$, the system with the reversed load model has eigenvalues

$$\lambda_{1,2} = -\frac{R}{L} \pm \sqrt{\frac{P^2+Q^2}{L^2\left(I_r^2+I_i^2\right)^2} - \frac{X^2}{L^2}} \tag{45}$$

$$\lambda_3 = -\frac{|\hat{I}|^2}{\tau G^2} \tag{46}$$

which represents the rapid convergence of G to a value which maintains constant power. The reversed load model with a fast time constant therefore represents the constant power load of Section III. If $\tau = 10^{-7}$ s, the system eigenvalues at equilibrium are

$$\lambda_1 = 3595.3 \quad \lambda_2 = -3673.5 \quad \lambda_3 = -9.7031 \times 10^6. \tag{47}$$

As in Section III, the fast reversed load model is unstable.

If the reversed load model has a time constant $\tau = 0.1$ s, the eigenvalues of (44) are

$$\lambda_{1,2} = -3702.4 \pm j375.91 \quad \lambda_3 = 9.2534. \tag{48}$$

These results indicate that while the phasor dynamics remain stable, the load conductance does not converge, making the system unstable. For $\tau \gg \tau_{ph}$, the system eigenvalues at equilibrium are approximately

$$\lambda_{1,2} = -\frac{R+G^{-1}}{L} \pm j\omega_0 \tag{49}$$

$$\lambda_3 = \frac{\left(I_r^2+I_i^2\right)\left[2(R+G^{-1}) - G((R+G^{-1})^2+X^2)\right]}{\tau G^3((R+G^{-1})^2+X^2)} \tag{50}$$

λ_3 is negative only if $G^{-2} < R^2 + X^2$. Since this condition is normally not true in typical power systems, the reversed dynamic load model does not appear to be stable for any value of τ in the infinite bus system of Fig. 1.

A more general dynamic model for PQ loads from [16] is also possible

$$\dot{G} = \frac{1}{\tau}\left[P - |\hat{I}|^2\frac{G}{G^2+B^2}\right] \tag{51}$$

$$\dot{B} = \frac{1}{\tau}\left[Q + |\hat{I}|^2\frac{B}{G^2+B^2}\right] \tag{52}$$

where both G and B are states. This model has performed very well in simulations by the authors, and we believe that its behavior is similar to the simplified model examined in this section, although we do not have a proof of stability.

Conventional dynamic load models, such as those used for studying voltage collapse [11], [12], are not necessarily suited for the study of phasor dynamics, in that these models are specified in terms of the real power of the load. For example, the load model in [12] may be written

$$\dot{x_L} = \frac{1}{T_P}[P_s(|\hat{V}_L|) - x_L P_t(|\hat{V}_L|)]. \tag{53}$$

Here x_L is the state variable, and $P_s(|\hat{V}_L|)$ and $P_t(|\hat{V}_L|)$ may in general be quadratic functions representing the steady-state and transient load models respectively. The real power being drawn by the load at any instant in time is $x_L P_t(|\hat{V}_L|)$. If $P_t(|\hat{V}_L|) = 1$, representing the transient load characteristic as a constant power model, then the transmission line dynamics will not in general be stable. To show this, note that the current dynamics are, from Section III (with $Q = 0$)

$$\dot{I}_r = \frac{1}{L}\left[V_{r1} - \frac{x_L I_r}{I_r^2+I_i^2} - RI_r + XI_i\right] \tag{54}$$

$$\dot{I}_i = \frac{1}{L}\left[V_{i1} - \frac{x_L I_i}{I_r^2 + I_i^2} - RI_i - XI_r\right]. \tag{55}$$

This system has a Jacobian of

$$\mathbf{A} = \begin{bmatrix} A_{11} & A_{12} & A_{13} \\ A_{21} & A_{22} & A_{23} \\ A_{31} & A_{32} & A_{33} \end{bmatrix} \tag{56}$$

$$A_{11} = \frac{\partial \dot{I}_r}{\partial I_r} = \frac{1}{L}\left[\frac{x_L\left(I_r^2 - I_i^2\right)}{\left(I_r^2 + I_i^2\right)^2} - R\right]$$

$$A_{12} = \frac{\partial \dot{I}_r}{\partial I_i} = \frac{1}{L}\left[\frac{2x_L I_r I_i}{\left(I_r^2 + I_i^2\right)^2} + X\right]$$

$$A_{13} = \frac{\partial \dot{I}_r}{\partial x_L} = -\frac{I_r}{L\left(I_r^2 + I_i^2\right)}$$

$$A_{21} = \frac{\partial \dot{I}_i}{\partial I_r} = \frac{1}{L}\left[\frac{2x_L I_r I_i}{\left(I_r^2 + I_i^2\right)^2} - X\right]$$

$$A_{22} = \frac{\partial \dot{I}_i}{\partial I_i} = \frac{1}{L}\left[\frac{x_L\left(I_i^2 - I_r^2\right)}{\left(I_r^2 + I_i^2\right)^2} - R\right]$$

$$A_{23} = \frac{\partial \dot{I}_i}{\partial x_L} = -\frac{I_i}{L\left(I_r^2 + I_i^2\right)}$$

$$A_{31} = \frac{\partial \dot{x}_L}{\partial I_r} = \frac{1}{T_P}\frac{\partial P_s(|\hat{V}_L|)}{\partial I_r}$$

$$A_{32} = \frac{\partial \dot{x}_L}{\partial I_i} = \frac{1}{T_P}\frac{\partial P_s(|\hat{V}_L|)}{\partial I_i}$$

$$A_{33} = \frac{\partial \dot{x}_L}{\partial x_L} = \frac{1}{T_P}\left[\frac{\partial P_s(|\hat{V}_L|)}{\partial x_L} - 1\right].$$

Note that the state x_L represents the instantaneous real power being drawn by the load. Typically, the time constant T_P has values ranging from a few seconds to many hours. Since $T_P \gg \tau_{ph}$, the dynamics of x_L will generally be much slower than the current dynamics, and hence the Jacobian of the system will have two eigenvalues nearly identical to equation (26). It was shown in Section III that one eigenvalue is positive under normal conditions.

The instability of this dynamic load model is clearly presented by inserting two common choices for the steady-state model. If the steady-state model is a constant power model $(P_s(|\hat{V}_L|) = P)$, then the load dynamic equation is

$$\dot{x_L} = \frac{1}{T_P}[P - x_L] \tag{57}$$

and therefore $A_{31} = A_{32} = 0$ and $A_{33} = -1/T_P$. Using the parameters from the earlier examples $(P = 1, x_L = 1)$ and $T_P = 1$ s, the eigenvalues of $\mathbf{A}$ are

$$\lambda_1 = 3598.1 \quad \lambda_2 = -3673.4 \quad \lambda_3 = -1. \tag{58}$$

If the static load model is a constant impedance with conductance G_s (i.e., $P_s(|\hat{V}_L|) = |\hat{V}_L|^2 G_s$), the stability conclusions are unchanged. Note that in this case, the load dynamics become

$$\dot{x_L} = \frac{1}{T_P}\left[\frac{x_L^2 G_s}{|\hat{I}|^2} - x_L\right] \tag{59}$$

since $\hat{V}_L\hat{I} = x_L$ at any instant in time. The third row of the Jacobian is now

$$A_{31} = \frac{\partial \dot{x}_L}{\partial I_r} = -\frac{2I_r x_L^2 G_s}{T_P\left(I_r^2 + I_i^2\right)^2}$$

$$A_{32} = \frac{\partial \dot{x}_L}{\partial I_i} = -\frac{2I_i x_L^2 G_s}{T_P\left(I_r^2 + I_i^2\right)^2}$$

$$A_{33} = \frac{\partial \dot{x}_L}{\partial x_L} = \frac{1}{T_P}\left[\frac{2x_L G_s}{I_r^2 + I_i^2} - 1\right].$$

Using the example parameters $(G_s = 1.0314)$ with a load time constant of 1 s, the eigenvalues are

$$\lambda_1 = 3600.1 \quad \lambda_2 = -3673.4 \quad \lambda_3 = -1.042. \tag{60}$$

However, if the dynamic load characteristic is changed to a constant impedance model $(P_t(|\hat{V}_L|) = |\hat{V}_L|^2)$, the state x_L represents the instantaneous conductance G of the load. Since $\hat{I} = \hat{V}_L G$ for all time, the system dynamics are identical to the model from [17] which was examined at the beginning of this section (for $P_s(|\hat{V}_L|) = P$).

V. Phasor Dynamics in a 3 Bus System

We now turn our attention to the 3-bus system shown in Fig. 3. Generator 1 is represented by a sixth-order two-axis model [18], [19], while generator 2 is treated as a slack bus. Because of the fast time scale of phasor dynamics, the stator dynamics of generator 1 are also included as described in Appendix A. Both constant impedance and constant PQ loads are considered, as well as the dynamic load of Section IV.

To analyze this example, we will select typical values for the system parameters, find the system equilibrium using load flow methods, and then examine the eigenvalues of the small-signal linear model around the equilibrium point. The generator parameters for the example considered are identical to those in [18]. The field voltage excitation will be constant at a value of $E_{fd} = 1.50537$. The network parameters are $R_{21} = R_{23} = R_{31} = 0.01, X_{21} = X_{23} = X_{31} = 0.1$, and $\hat{V}_3 = 1\angle 0°$.

Beginning with a constant impedance load of resistance $R_L = 0.9873$ and zero reactance, the equilibrium for the system occurs at $\hat{V}_1 = 0.9936\angle -2.89°$ and $\hat{V}_2 = 0.9999\angle -0.009°$. At equilibrium, the load draws 1 p.u. of real power, so that a constant PQ load with $P = 1$ and $Q = 0$ will produce the same load flow solution (and same equilibrium point) as the constant impedance.

The eigenvalues of the system at equilibrium with a constant impedance load are given in Table I, while the system eigenvalues with a PQ load are shown in Table II. Again, we see that the system with a constant impedance load is stable, while the system with a PQ load is not. Fig. 4 illustrates the response of the dynamics of the system with a PQ load when starting at the load flow solution point given above.

When the dynamic load is used, the results are similar. A long time constant ($\tau = 0.1$ s) results in a stable system, as shown in Table III. These eigenvalues are nearly identical to Table I, with the addition of one mode which represents the load dynamics. For a relatively slowly varying load conductance, the load resembles a constant impedance with respect to the phasor dynamics. If a short time constant is used with the reversed load

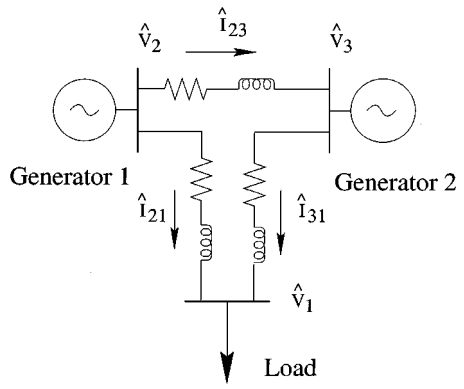

Fig. 3. Three bus system for analysis of phasor dynamics.

TABLE I
EIGENVALUES AND FREQUENCIES OF THE LINEARIZED SYSTEM WITH A CONSTANT IMPEDANCE LOAD

Number(s)	Eigenvalue	Frequency (Hz)
1,2	$-5886 \pm j377.0$	59.99
3,4	$-37.70 \pm j377.0$	60.00
5,6	$-6.830 \pm j376.7$	59.96
7	-40.57	–
8	-38.71	–
9,10	$-1.703 \pm j9.677$	1.540
11	-4.781	–
12	-0.3366	–

TABLE II
EIGENVALUES AND FREQUENCIES OF THE LINEARIZED SYSTEM WITH A CONSTANT POWER LOAD

Number(s)	Eigenvalue	Frequency (Hz)
1	5880	–
2	-5874	–
3,4	$-37.70 \pm j377.0$	60.00
5,6	$-6.838 \pm j376.7$	59.96
7	-40.55	–
8	-38.73	–
9,10	$-1.705 \pm j9.676$	1.540
11	-4.782	–
12	-0.3364	–

model ($\tau = 10^{-7}$ s), the resulting system is unstable (Table IV). This result shows that the fast dynamic load is very similar to the constant power load.

Note that the dynamics of the 3-bus system include several different time-scales, ranging from the very fast transmission line dynamics to the slow dynamics in the generator. Using selective modal analysis [20] we find that eigenvalues 1–4 correspond to the fast dynamics of the transmission lines. Eigenvalues 5–12 all correspond to the dynamics of generator 1. Eigenvalues 5 and 6 represent the dynamics in the stator of generator 1, which are slower because of low resistance and high inductance in the armature winding and the network. Eigenvalues 7 and 8 indicate the subtransient dynamics, 11 and 12 represent the transient dynamics, and 9 and 10 represent

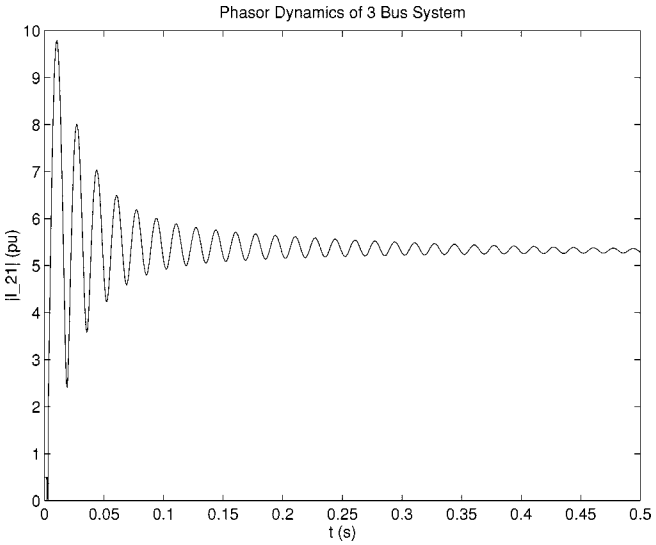

Fig. 4. Magnitude of line current 21 in the 3 bus system.

TABLE III
EIGENVALUES AND FREQUENCIES OF THE LINEARIZED SYSTEM WITH A DYNAMIC LOAD ($\tau = 0.1$ s)

Number(s)	Eigenvalue	Frequency (Hz)
1,2	$-5876 \pm j377.5$	60.07
3,4	$-37.70 \pm j377.0$	60.00
5,6	$-6.830 \pm j376.7$	59.96
7	-40.58	–
8	-38.71	–
9,10	$-1.704 \pm j9.678$	1.540
11	-4.782	–
12	-0.3364	–
13	-9.698	–

TABLE IV
EIGENVALUES AND FREQUENCIES OF THE LINEARIZED SYSTEM WITH A REVERSED DYNAMIC LOAD ($\tau = 10^{-7}$ s)

Number(s)	Eigenvalue	Frequency (Hz)
1	5793	–
2	-5874	–
3,4	$-37.70 \pm j377.0$	60.00
5,6	$-6.838 \pm j376.7$	59.96
7	-40.55	–
8	-38.73	–
9,10	$-1.705 \pm j9.676$	1.540
11	-4.782	–
12	-0.3364	–
13	-9.885×10^6	–

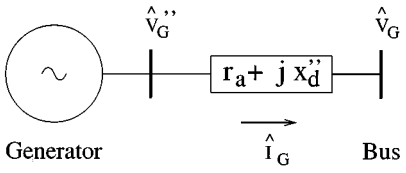

Fig. 5. Equivalent representation of stator dynamics.

the mechanical dynamics. Finally, eigenvalue 13 represents the dynamics of the load.

The instability that is observed here for a PQ load occurs on a fast time scale. The singular perturbations assumption of reducing the fastest dynamics to an algebraic relation [21] is not valid here for a PQ load, because these dynamics on the fastest time scale are unstable and do not converge to the normal equilibrium point.

VI. Conclusion

In this paper, we have added the transmission line dynamics that are normally ignored in power systems analysis. The addition of these dynamics leads to some new conclusions. A constant impedance load model is not seen to cause any instabilities in the network current dynamics; however, the use of a constant PQ model is indeed shown to produce such instabilities around the load flow solution point of interest. Dynamic load models based on a slowly varying constant power model exhibit similar behavior. Therefore, we conclude that on the time scale of phasor dynamics, a constant power load model is not a valid assumption; instead, load models which capture the fast dynamics are needed. It is hard to quantify the frequency ranges within which it would be essential to have dynamic load representation. However, based on our analysis here it appears that for frequency ranges and phenomena (such as subsynchronous resonance [4]) in which dynamics of transmission lines are relevant, the same would be the case with the load representation. With the development of FACTS devices and other transmission network enhancements, this issue of consistent load modeling for proper analysis of fast network dynamics becomes particularly important.

Note: The authors wish to acknowledge the contribution of (23), (24), and (27) from one of the reviewers.

Appendix I
Stator Dynamics

The stator dynamics[2] of a generator may be expressed in terms of fluxes ψ_d and ψ_q [3], [22]

$$\frac{d\psi_d}{dt} = \omega_o e_d + \omega\psi_q + \omega_o r_a i_d \tag{61}$$

$$\frac{d\psi_q}{dt} = \omega_o e_q - \omega\psi_d + \omega_o r_a i_q \tag{62}$$

where r_a is armature resistance and $e_d + je_q$ and $i_d + ji_q$ are terminal voltage and current, respectively, in the machine frame of reference. Machine current is related to flux by [22]

$$i_d = \frac{e''_q - \psi_d}{x''_d} \tag{63}$$

$$i_q = \frac{-e''_d - \psi_q}{x''_q}. \tag{64}$$

[2]This appendix is added in response to one of the reviewer's requests to investigate the impact of stator dynamics on conclusions in this paper. As it turns out, there is no ready to use reference for this purpose, particularly when analyzing interplay of the network and stator phasor dynamics. Consequently, new derivations are provided in this Appendix.

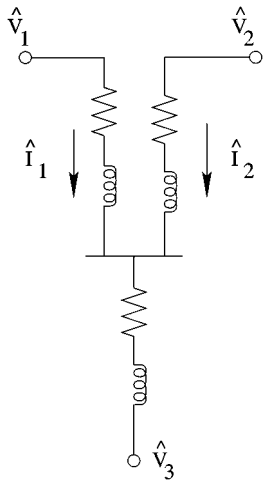

Fig. 6. Diagram of three inductive impedances in a "Y" connection.

We can now use i_d and i_q as state variables by differentiating these last two equations and substituting (61) and (62) for the flux derivatives

$$\frac{di_d}{dt} = \frac{1}{x''_d}[\dot{e}''_q - \omega_o e_d + \omega(e''_d + x''_q i_q) - \omega_o r_a i_d] \tag{65}$$

$$\frac{di_q}{dt} = \frac{1}{x''_q}[-\dot{e}''_d - \omega_o e_q + \omega(e''_q - x''_d i_d) - \omega_o r_a i_q]. \tag{66}$$

Assuming no subtransient saliency ($x''_d = x''_q$), we can now use as state variables the current in the network frame of reference (denoted henceforth as $\hat{I}_G = I_{Gr} + jI_{Gi}$) by applying an inverse Park transform

$$I_{Gr} = i_d \sin\delta + i_q \cos\delta \tag{67}$$

$$I_{Gi} = -i_d \cos\delta + i_q \sin\delta. \tag{68}$$

The time derivatives of network current are then

$$\dot{I}_{Gr} = \frac{di_d}{dt}\sin\delta + \frac{di_q}{dt}\cos\delta - (\omega - \omega_o) I_{Gi} \tag{69}$$

$$\dot{I}_{Gi} = -\frac{di_d}{dt}\cos\delta + \frac{di_q}{dt}\sin\delta + (\omega - \omega_o) I_{Gr}. \tag{70}$$

Substituting (65) and (66)

$$\dot{I}_{Gr} = \frac{\omega_o}{x''_d}[V''_{Gr} - V_{Gr} - r_a I_{Gr} + x''_d I_{Gi}] \tag{71}$$

$$\dot{I}_{Gi} = \frac{\omega_o}{x''_d}[V''_{Gi} - V_{Gi} - r_a I_{Gi} - x''_d I_{Gr}] \tag{72}$$

$$V''_{Gr} = \left(\frac{\omega}{\omega_o} e''_d + \frac{\dot{e}''_q}{\omega_o}\right)\sin\delta + \left(\frac{\omega}{\omega_o} e''_q - \frac{\dot{e}''_d}{\omega_o}\right)\cos\delta \tag{73}$$

$$V''_{Gi} = -\left(\frac{\omega}{\omega_o} e''_d + \frac{\dot{e}''_q}{\omega_o}\right)\cos\delta + \left(\frac{\omega}{\omega_o} e''_q - \frac{\dot{e}''_d}{\omega_o}\right)\sin\delta \tag{74}$$

$$V_{Gr} = e_d \sin\delta + e_q \cos\delta \tag{75}$$

$$V_{Gi} = -e_q \cos\delta + e_d \sin\delta. \tag{76}$$

The stator dynamics given by these equations can be represented by the equivalent circuit in Fig. 5. These dynamics are equivalent to the phasor dynamics of an impedance $r_a + jx''_d$ with a voltage difference of $\hat{V}''_G - \hat{V}_G$. $\hat{V}_G = V_{Gr} + jV_{Gi}$ is the generator terminal voltage, while $\hat{V}''_G = V''_{Gr} + jV''_{Gi}$ is a function of the subtransient states.

Since the generators in the three bus example are connected to two transmission lines, the stator dynamics produce a "Y" connection of three inductive impedances as shown in Fig. 6. The dynamics of the "Y" connection may be written in state-space form by choosing two of the line currents (here $\hat{I}_1$ and $\hat{I}_2$) as states. Then, using the basic circuit element equations

$$\hat{V}_1 = \hat{V}_3 + \hat{Z}_3(\hat{I}_1 + \hat{I}_2) + L_3\frac{d(\hat{I}_1 + \hat{I}_2)}{dt} + \hat{Z}_1\hat{I}_1 + L_1\frac{d\hat{I}_1}{dt} \tag{77}$$

$$\hat{V}_2 = \hat{V}_3 + \hat{Z}_3(\hat{I}_1 + \hat{I}_2) + L_3\frac{d(\hat{I}_1 + \hat{I}_2)}{dt} + \hat{Z}_2\hat{I}_2 + L_2\frac{d\hat{I}_2}{dt}. \tag{78}$$

This is a system of two equations with two unknowns (the derivatives of $\hat{I}_1$ and $\hat{I}_2$). Solving for these derivatives gives

$$\frac{d\hat{I}_1}{dt} = \frac{L_2(\hat{V}_1 - \hat{V}_3 - \hat{Z}_1\hat{I}_1 - \hat{Z}_3(\hat{I}_1 + \hat{I}_2))}{L_1L_2 + L_3(L_1 + L_2)} + \frac{L_3(\hat{V}_1 - \hat{V}_2 - \hat{Z}_1\hat{I}_1 + \hat{Z}_2\hat{I}_2)}{L_1L_2 + L_3(L_1 + L_2)} \tag{79}$$

$$\frac{d\hat{I}_2}{dt} = \frac{L_1(\hat{V}_2 - \hat{V}_3 - \hat{Z}_2\hat{I}_2 - \hat{Z}_3(\hat{I}_1 + \hat{I}_2))}{L_1L_2 + L_3(L_1 + L_2)} + \frac{L_3(\hat{V}_2 - \hat{V}_1 - \hat{Z}_2\hat{I}_2 + \hat{Z}_1\hat{I}_1)}{L_1L_2 + L_3(L_1 + L_2)}. \tag{80}$$

The combination of the stator equivalent impedance and the "Y" connection dynamics are used to represent the stator dynamics.

REFERENCES

[1] D. Hill, I. Hiskens, and I. Mareels, "Stability theory of differential/algebraic models of power systems," in *Proc. 11th Triennial World Congr. IFAC*, vol. VI, Tallinn, USSR, Aug. 13–17, 1990, pp. 19–24.

[2] J. Zaborszky, H. Schättler, and V. Venkatasubramanian, "Error estimation and limitation of the quasi stationary phasor dynamics," in *Proc. 11th Power Systems Computation Conf.*, Avignon, France, 1993, pp. 721–729.

[3] M. Ilić and J. Zaborszky, Dynamics and Control of the Large Electric Power Systems, Wiley (Interscience Division), 2000.

[4] E. Allen, J. Chapman, and M. Ilić, "Effects of torsional dynamics on nonlinear generator control," *IEEE Trans. Contr. Syst. Technol.*, vol. 4, pp. 125–140, Mar. 1996.

[5] C. DeMarco and G. Verghese, "Bringing phasor dynamics into the power system load flow," presented at the Proc. 25th North American Power Symp., 1993.

[6] V. Venkatasubramanian, H. Schättler, and J. Zaborszky, "A time-delay differential-algebraic phasor analysis of the large power system dynamics," in *Proc. ISCAS*, vol. 6, May 1994, pp. 49–52.

[7] V. Venkatasubramanian, X. Jiang, H. Schättler, and J. Zaborszky, "Current status of the taxonomy theory of power system dynamics: Constrained systems with hard limits," in *Proc. NSF Inter. Workshop Bulk Power Voltage Phenomena*, Davos, Switzerland, Aug. 1994, pp. 15–103.

[8] V. Venkatasubramanian, H. Schättler, and J. Zaborszky, "Fast time-varying phasor analysis in the balanced three phase large electric power system," *IEEE Trans. Automat. Contr.*, vol. AC-40, pp. 1975–1982, Nov. 1995.

[9] D. Hill, "On the equilibria of power systems with nonlinear loads," *IEEE Trans. Circuits Syst.*, vol. 36, pp. 1458–1463, 1989.

[10] "Load representation for dynamic performance analysis," *IEEE Trans. Power Syst.*, vol. 8, pp. 472–482, 1993. IEEE Task Force on Load Representation for Dynamic Performance.

[11] D. Hill, "Nonlinear dynamic load models with recovery for voltage stability studies," *IEEE Trans. Power Syst.*, vol. 8, pp. 166–176, 1993.

[12] W. Xu and Y. Mansour, "Voltage stability analysis using generic dynamic load models," *IEEE Trans. Power Syst.*, vol. 9, pp. 479–493, 1994.

[13] P. Anderson, B. Agrawal, and J. Van Ness, *Subsynchronous Resonance in Power Systems*, N.Y.: IEEE Press, 1990.

[14] C. Bowler, D. Ewart, and C. Concordia, "Self excited torsional frequency oscillations with series capacitors," *IEEE Trans. Power Apparatus and Systems*, vol. PAS-92, pp. 1688–1695, 1973.

[15] E. Allen, J. Chapman, and M. Ilić, "Eigenvalue analysis of the stabilizing effects of feedback linearizing control on subsynchronous resonance," in *Proc. 4th IEEE Conf. Contr. Appli.*, Albany, NY, Sept. 28–29, 1995, pp. 395–402.

[16] E. Allen, N. LaWhite, Y. Yoon, J. Chapman, and M. Ilić, "Interactive object-oriented simulation of interconnected power systems using SIMULINK," in *Proc. 27th An. North American Power Symp.*, Bozeman, MT, Oct. 2–3, 1995, pp. 235–243.

[17] M. K. Pal, "Voltage stability conditions considering load characteristics," *IEEE Trans. Power Syst.*, vol. 7, pp. 243–249, 1992.

[18] J. W. Chapman *et al.*, "Stabilizing a multimachine power system via decentralized feedback linearizing control," *IEEE Trans. Power Syst.*, vol. 8, pp. 830–839, 1993.

[19] R. Schulz, Synchronous machine modeling, , IEEE Publication 75 CH0970-4-PWR, 1975.

[20] I. J. Pérez-Arriaga, G. C. Verghese, and F. C. Schweppe, "Selective modal analysis with applications to electric power systems, part I: Heuristic introduction," *IEEE Trans. Power Apparatus and Syst.*, vol. PAS-101, pp. 3117–3134, 1982.

[21] P. Kokotović, H. K. Khalil, and J. O'Reilly, *Singular Perturbation Methods in Control: Analysis and Design*. Orlando, FL: Academic, 1986.

[22] J. Kirtley Jr., Synchronous machine dynamic models, , Massachusetts Institute of Technology, Apr. 5, 1993. 6.685 Class Notes.

Eric H. Allen received the B.S. degree in electrical engineering from Worcester Polytechnic Institute in 1993. He received the S.M. degree in electrical engineering from the Massachusetts Institute of Technology in 1995, studying the effects of torsional shaft dynamics on nonlinear generator excitation control. In 1998 he received the Ph.D. degree in the field of electrical engineering from M.I.T.

He is currently working at the NY Indepedent System Operator (ISO) in the planning division. His research interests include dynamic systems and control in electric power systems, dynamic programming for commitment decisions in electricity markets, and stochastic control.

Marija D. Ilić is a Senior Research Scientist in the Department of Electrical Engineering and Computer Science at M.I.T. where she teaches several graduate courses in the area of electric power systems and heads research in the same area. She has over 20 years of experience in teaching and doing research in this area. Prior to coming to M.I.T. in 1987, she was an Assistant Professor at Cornell University, and tenured Associate Professor at the University of Illinois at Urbana-Champaign. She is a co-author of the book entitled *Hierarchical Power Systems Control: Its Value in a Changing Industry*, and a co-editor of the book entitled *Electric Power Systems Restructuring: Engineering and Economics* Most recently, she has co-authored a major textbook entitled *Dynamics and Control of Large Electric Power Systems*. Her main research interest is in the networks and systems aspects of operations, planning and economics of electric power industry.